

Multimodal mapping of regional brain vulnerability to focal cortical dysplasia

Hyo M. Lee,¹ Seok-Jun Hong,^{1,2} Ravnoor Gill,¹ Benoit Caldaïrou,¹ Irene Wang,³ Jian-guo Zhang,⁴ Francesco Deleo,⁵ Dewi Schrader,⁶ Fabrice Bartolomei,⁷ Maxime Guye,⁸ Kyoo Ho Cho,⁹ Carmen Barba,¹⁰ Sanjay Sisodiya,¹¹ Graeme Jackson,¹² R. Edward Hogan,¹³ Lily Wong-Kisiel,¹⁴ Gregory D. Cascino,¹⁴ Andreas Schulze-Bonhage,¹⁵ Iscia Lopes-Cendes,¹⁶ Fernando Cendes,¹⁶ Renzo Guerrini,¹⁷ Boris Bernhardt,¹⁸ Neda Bernasconi¹ and Andrea Bernasconi¹

Abstract

Focal cortical dysplasia (FCD) type II is a highly epileptogenic developmental malformation and a common cause of surgically treated drug-resistant epilepsy. While clinical observations suggest frequent occurrence in the frontal lobe, mechanisms for such propensity remain unexplored. Here, we hypothesized that cortex-wide spatial associations of FCD distribution with cortical cytoarchitecture, gene expression and organizational axes may offer complementary insights into processes that predispose given cortical regions to harbor FCD.

We mapped the cortex-wide MRI distribution of FCDs in 337 patients collected from 13 sites worldwide. We then determined its associations with 1) cytoarchitectural features using histological atlases by Von Economo and Koskinas and BigBrain, 2) whole-brain gene expression and spatiotemporal dynamics from prenatal to adulthood stages using the Allen Human Brain Atlas and PsychENCODE BrainSpan and 3) macroscale developmental axes of cortical organization.

FCD lesions were preferentially located in the prefrontal and fronto-limbic cortices typified by low neuron density, large soma and thick gray matter. Transcriptomic associations with FCD distribution uncovered a prenatal component related to neuroglial proliferation and differentiation, likely accounting for the dysplastic makeup, and a postnatal component related to synaptogenesis and circuit organization, possibly contributing to circuit-level hyperexcitability. FCD distribution showed a strong association with the anterior region of the antero-posterior axis derived from heritability analysis of inter-regional structural covariance of cortical thickness, but not with structural and functional hierarchical axes. Reliability of all results was confirmed through resampling techniques.

1 Multimodal associations with cytoarchitecture, gene expression and axes of cortical
2 organization indicates that prenatal neurogenesis and postnatal synaptogenesis may be key points
3 of developmental vulnerability of the frontal lobe to FCD. Concordant with a causal role of atypical
4 neuroglial proliferation and growth, our results indicate that FCD-vulnerable cortices display
5 properties indicative of earlier termination of neurogenesis and initiation of cell growth. They also
6 suggest a potential contribution of aberrant postnatal synaptogenesis and circuit development to
7 FCD epileptogenicity.

8 9 **Author affiliations**

10 1 Neuroimaging of Epilepsy Laboratory, Montreal Neurological Institute, McGill University,
11 Montreal, Canada

12 2 Center for Neuroscience Imaging, Research Institute for Basic Science, Department of Global
13 Biomedical Engineering, SungKyunKwan University, Suwon, Korea Suwon, Korea

14 3 Epilepsy Center, Neurological Institute, Cleveland Clinic, Cleveland, OH, USA

15 4 Department of Functional Neurosurgery, Beijing Tiantan Hospital, Capital Medical University,
16 Beijing, China

17 5 Epilepsy Unit, Fondazione IRCCS Istituto Neurologico C. Besta, Milano, Italy

18 6 Department of Pediatrics, British Columbia Children's Hospital, Vancouver, Canada

19 7 Aix Marseille Univ, INSERM, INS, Institut de Neurosciences des Systèmes, Marseille, 13005,
20 France

21 8 Aix Marseille University, CNRS, CRMBM UMR 7339, Marseille, France

22 9 Department of Neurology, Yonsei University College of Medicine, Seoul, Korea

23 10 Neuroscience Department, Children's Hospital A. Meyer-University of Florence, Italy

24 11 Department of Clinical and Experimental Epilepsy, UCL Queen Square Institute of Neurology,
25 London, UK

26 12 The Florey Institute of Neuroscience and Mental Health and The University of Melbourne,
27 Victoria, Australia

1 13 Department of Neurology, Washington University School of Medicine, St Louis, Missouri,
2 USA

3 14 Mayo Clinic, Department of Neurology, Rochester, MN, USA

4 15 Epilepsy Center, University Medical Center-University of Freiburg, Freiburg, Germany

5 16 Department of Translational Medicine, School of Medical Sciences, University of Campinas
6 (UNICAMP) and the Brazilian Institute of Neuroscience and Neurotechnology (BRAINN),
7 Campinas SP, Brazil

8 17 Department of Neurology, School of Medical Sciences, University of Campinas (UNICAMP),
9 and the Brazilian Institute of Neuroscience and Neurotechnology (BRAINN), Campinas SP, Brazil

10 18 Multimodal Imaging and Connectome Analysis Lab, McConnell Brain Imaging Centre,
11 Montreal Neurological Institute and Hospital, McGill University, Montreal, QC, Canada

12

13 Correspondence to: Andrea Bernasconi, MD

14 Montreal Neurological Institute and Hospital

15 McGill University

16 3801 University Street

17 Montreal, Quebec, Canada H3A 2B4

18 E-mail: andrea.bernasconi@mcgill.ca

19

20 **Running title:** Developmental vulnerability for FCD

21 **Keywords:** focal cortical dysplasia; MRI; epilepsy; neurodevelopment; imaging-genetics

22

23 **Introduction**

24 Focal cortical dysplasia (FCD) type II is the most prevalent epileptogenic developmental brain
25 malformation and a common cause of surgically amenable epilepsy.¹ This lesion is characterized

1 by cortical dyslamination, cytomegaly and cortical thickening,² likely due to atypical neuroglial
2 proliferation, growth and migration.³ At a molecular scale, studies in resected FCD tissue have
3 established a causal role of somatic mutations in genes implicated in the mechanistic target of the
4 rapamycin (mTOR) pathway⁴⁻⁷; mTOR hyperactivity disrupts neuronal migration and cortical
5 lamination.⁷ A recent multiomic study of somatic mutations in hemimegalencephaly and FCD also
6 implicated genes related to calcium dynamics and synaptic function as potential contributors to
7 epileptogenesis.⁸

8 Although FCD type II lesions may occur across the entire cortex, histopathological reports of
9 surgically resected tissues in large cohorts^{1, 9, 10} as well as a recent atlas of lesion location,¹¹ suggest
10 a propensity for frontal lobe involvement. However, mechanisms underpinning this regional
11 vulnerability remain unexplored. Notably, the developing cortex undergoes area-specific,
12 genetically regulated neurogenesis, synaptogenesis and circuit development that give rise to
13 variations in cytoarchitecture.¹² Given the strong genetic influence on regional cytoarchitecture,¹³
14 it is conceivable that architectural features of the putative FCD-prone cortices may inform on the
15 morphopathogenic characteristics of this malformation.¹⁴ Likewise, given the substantial
16 variability of gene expression profiles across the cortex,¹⁵ their relation to FCD topology may
17 provide insights into the molecular pathways contributing to the pathogenesis of this brain
18 malformation. Furthermore, cortical organization is thought to be governed by graded macroscale
19 axes, emerging from gene expression,^{12, 16, 17} morphology and microstructure¹⁸⁻²¹ as well as
20 functional and structural connectivity.^{22, 23} Specifically, the antero-posterior axis related to the
21 prenatal timetable of neuroglial proliferation and growth,²⁴⁻²⁶ results in a gradient of neuronal
22 density, size and cortical thickness that persists throughout adulthood.^{13, 20, 27} Another increasingly
23 recognized axis marks the transition from sensory to transmodal association cortices.^{17, 21, 23, 28, 29}
24 Recapitulating classic accounts formulated in non-human primates,³⁰ this axis has been thought to
25 mature during late prenatal and early postnatal stages³¹ and reflect the hierarchical organization of
26 neural function. In sum, cortex-wide spatial associations of FCD distribution with cortical
27 cytoarchitecture, gene expression and organizational axes may offer complementary insights into
28 the neurogenic processes that predispose given cortical regions to harbor this developmental
29 malformation.^{14, 29}

30 Whole-brain cross-modal associations are facilitated by the availability of human brain atlases
31 based on histological features³²⁻³⁴ and spatiotemporal gene expression profiles.^{35, 36} The overall

1 purpose of this work was to investigate the intrinsic regional vulnerability of cortices harboring
2 FCD. To this end, we mapped the cortex-wide lesional distribution of a multicentric dataset
3 collected from epilepsy centers worldwide, determined cellular and genetic factors based on
4 postmortem histology and transcriptomics, and examined the embedding of FCD lesions within
5 the axes of neurogenic patterning and structure-function hierarchy. Specifically, after creating a
6 topographic map of FCD type II lesions on MRI-derived cortical surface models, we cross-
7 referenced it against histological taxonomies^{32, 33} and a 3D high-resolution human brain
8 histological model.³⁴ In parallel, we performed spatial correlation with whole-brain gene
9 expression data from the Allen Human Brain Atlas³⁵ and examined spatiotemporal gene expression
10 dynamics from prenatal to adulthood stages using the PsychENCODE BrainSpan, an independent
11 development-targeted genetic dataset.^{36, 37} Targeted gene enrichment analysis probed
12 transcriptomic associations for previously known pathogenic FCD variants,^{3, 38, 39} as well as non-
13 FCD epilepsies⁴⁰ and other neurological disorders. Finally, we contextualized the FCD distribution
14 within the antero-posterior axis previously associated with genetic cortical patterning and
15 timetable of neurogenesis,^{13, 24-26} contrasting these findings with hierarchical cortical axes derived
16 from myelin-sensitive MRI²⁸ and resting-state MRI functional connectivity.²³

17

18 **Materials and methods**

19 **Study design and participants**

20 We studied a consecutive retrospective cohort of 337 patients (153 females; mean±SD age =
21 22.2±12.7 years) with histologically verified FCD lesions collected from 13 tertiary epilepsy
22 centers worldwide. All patients had been investigated for drug-resistant epilepsy with a standard
23 presurgical workup including assessment of seizure history, routine MRI and video-EEG
24 recordings. Histological examination of the surgical specimen² determined FCD type II as
25 disrupted cortical lamination with dysmorphic neurons in isolation (IIA, n=134) or together with
26 balloon cells (IIB, n=203). Site-specific demographics are summarized in **Table 1**. The Ethics
27 Committees and Institutional Review Boards at all participating sites approved the study, and
28 written informed consent was obtained from all patients.

29

1 **MRI acquisition and processing**

2 All patients had high-resolution 3D T1-weighted MRI (T1w) acquired as a part of the clinical
3 presurgical investigation, consisting of images with isotropic 1x1x1 mm voxel resolution.⁴¹ Data
4 underwent intensity non-uniformity correction and normalization, and linear registration to the
5 ICBM MNI152 symmetric template. To generate cortical surface models, we applied the
6 Constrained Laplacian Anatomic Segmentation using Proximity algorithm, yielding GM-WM and
7 GM-CSF surfaces with 41k surface points (or vertices) per hemisphere.⁴² Surface-based
8 registration, which aligns individual participants based on cortical folding, was performed to
9 optimize vertex-wise anatomical correspondence across participants.⁴³

10

11 **Cortex-wide MRI mapping of FCD lesions**

12 Two experts (AB, NB) independently segmented each FCD lesion on the 3D MRI registered onto
13 the ICBM MNI152 template. The consensus labels (the union of the two segmentations; inter-rate
14 Dice index: 0.94 ± 0.13) was intersected with the cortical surfaces to generate surface-based FCD
15 labels. To enhance regional sensitivity while retaining specificity, labels were minimally smoothed
16 using a surface-based 4 mm full width at half maximum Gaussian kernel to maximize local
17 specificity.⁴⁴ We then calculated for each vertex the FCD probability, defined as the percentage of
18 patients whose lesion label coincided with that vertex. To assess *within-sample* reliability, we
19 calculated bootstrap certainty at each vertex, defined by mean of lesion probability from the
20 bootstrap subsamples divided by their standard deviation. Similarly, we assessed *cross-site*
21 reliability as defined by the mean divided by the standard deviation from leave-one-site-out
22 subsamples. We assessed the lobar distribution by counting the number of FCD lesions located
23 within each lobe; to account for lobar size, we divided the lesion counts by the relative surface
24 areas of each lobe, defined based on automated anatomical labelling parcellation atlas.⁴⁵

25

26

1 **Association analyses**

2 **Histological atlases**

3 To assess associations of regional FCD probability with histological markers, we used the von
4 Economo-Koskinas MRI atlas (<http://dutchconnectomelab.nl>) indexed with quantitative
5 histological information (cell size, cell density and cortical thickness) of 43 cortical regions per
6 hemisphere.³³ For independent validation, we leveraged the BigBrain atlas, a 3D reconstruction of
7 a stained post-mortem human brain³⁴; this histological data, mapped to intracortical surface models
8 in standard space and to the Schaefer 400 parcellations,⁴⁶ were obtained from
9 <https://github.com/MICA-MNI/micaopen/tree/master/bigbrain>.

10

11 **Cortex-wide gene expression**

12 To investigate the molecular properties of cortical vulnerability, we related the FCD distribution
13 with the anatomically comprehensive gene expression data from Allen Human Brain Atlas
14 (AHBA; six postmortem adult brains; 1 female; age = 42.5±13.4 years; [https://human.brain-
15 map.org](https://human.brain-map.org)),³⁵ which was mapped onto the 308 parcels of the Desikan-Killiany atlas (DKA).⁴⁷ The
16 microarray data of these donors were acquired using ~500 samples per hemisphere, with each
17 sample indexed with expression levels for ~60,000 genes from at least two probes. Following an
18 established procedure,⁴⁸ the Maybrain package (<https://github.com/rittman/maybrain>) matched the
19 closest AHBA sample in each donor to the centroids of 308 parcels of equal area (500 mm²)
20 averaged across donors. Notably, data were averaged across probes corresponding to the same
21 gene, excluding those not matched to gene symbols in the AHBA data. To reduce inter-donor
22 variability, expression data for each probe were normalized through z-transformations across the
23 308 DKA parcels within each donor. The final output was a matrix of z-scored expression values
24 for each of 20,737 genes mapped onto the 308 DKA parcels.

25

26 **Spatiotemporal gene expression**

27 We determined how genes associated with the FCD distribution are spatially and temporally
28 regulated throughout the pre- and postnatal development. To this purpose, we used

1 PsychENCODE BrainSpan (<http://development.psychencode.org>),³⁶ a dataset including tissue-
2 level mRNA-sequencing of 607 samples across 16 anatomical brain regions of 41 postmortem
3 human brains ranging from 8 postconceptional weeks to 40 postnatal years (18 females;
4 postmortem interval = 12.9 ± 10.4 hours; tissue pH = 6.5 ± 0.3 ; RNA integrity number = 8.8 ± 1).
5 After bulk tissue mRNA-sequencing, this dataset has yielded expression levels for 60,154 genes.
6 The final output consisted of a matrix of reads per kilobase million transcript expression level for
7 each of 17,584 genes overlapping with the 20,737 genes from the AHBA atlas.

8

9 **Developmental axes of cortical network organization**

10 Gradient axes of cortical structural and functional network organization are shaped by gene
11 expression and cytoarchitecture during the pre- and postnatal development. The antero-posterior
12 axis relates to the prenatal timetable of neurogenesis and growth²⁴⁻²⁶; we derived this axis from a
13 heritability analysis of structural covariance networks¹³ mapped on the Schaefer 400
14 parcellations.⁴⁶ Structural and functional hierarchical axes are thought to mature during late
15 prenatal and early postnatal circuit development³¹; we derived these axes from MRI-based
16 covariance of microstructural profiles²⁸ and resting-state functional connectivity,²³ which we
17 mapped to the Schaefer 400 parcellations using the BrainSpace toolbox
18 (<https://github.com/MICA-MNI/BrainSpace>).⁴⁹ The FCD distribution and developmental axes
19 were mapped to Schaefer 400 parcellations prior to correlation analysis to achieve anatomical
20 correspondence between them.

21

22 **Statistical analysis**

23 **Multivariate analysis**

24 Cortex-wide linear models assessed associations of regional FCD probability with histological
25 markers and neurodevelopmental axes. For the gene expression analysis, given the high
26 dimensionality of AHBA data, we used partial least squares (PLS) regression, a multivariate linear
27 model, to uncover weighted combinations of genes (or PLS components) that best explained the
28 regional variance in FCD probability. The statistical significance of the variance explained by the

1 PLS components was tested based on 10,000 spin permutations of the FCD distribution,
2 accounting for spatial autocorrelations.⁵⁰ The regional expression profile of each PLS component
3 was defined as the average of the spatial expression profile of 20,757 genes, adjusted by their PLS
4 weight; weight stability was estimated by dividing the PLS weight by the bootstrap SD.

6 **Enrichment analysis**

7 A web-based gene set analysis toolkit (<https://webgestalt.org>)⁵¹ was utilized to uncover biological
8 processes enriched in the list of genes whose bootstrap weights (absolute value) were ranked
9 within the top 10 percentile of 20,757 genes. In other words, this analysis quantified the
10 significance and enrichment ratio, namely the number of PLS-derived genes overlapping with each
11 biological process divided by the number of genes expected to overlap by random permutations.

13 **Spatiotemporal gene expression profiles**

14 Using the PsychENCODE BrainSpan dataset, we calculated the spatiotemporal profile for each
15 PLS component obtained in the gene expression analysis. This profile, defined as the regional
16 average of each gene's expression level weighted by its bootstrap weight, was obtained across 16
17 cortical regions and timepoints based on major neurodevelopmental milestones derived from
18 whole-brain transcriptomic signatures.⁵² Student's t-tests compared the expression levels between
19 time windows, and between different regions within time windows.

21 **Specificity analysis**

22 We assessed whether known genes of the pathways causing FCD via somatic mutations were
23 enriched in the PLS components, including the PI3K-AKT-mTOR pathway,^{5, 6, 38, 53, 54} PI3K-
24 PTEN-AKT-TSC-RHEB pathway,^{6, 53, 55-57} TSC1-TSC2 complex,⁵⁸⁻⁶¹ GATOR1 complex^{6, 55, 57, 59,}
25 ⁶²⁻⁶⁵ and other reported variants (IRS1, RAB6B, ZNF337, RALA and HTR6).⁶¹ These genes are
26 listed in **Supplementary Table 1**. We also assessed associations with risk genes of focal epilepsy
27 with hippocampal sclerosis, generalized epilepsy and all epilepsies as determined by a recent
28 genome-wide association study,⁴⁰ neurodevelopmental conditions, namely autism⁶⁶ and bipolar

1 spectrum.⁶⁷ Finally, our specificity analysis included frontotemporal dementia⁶⁸ due to the
2 preferential involvement of the frontal lobe.

3 For each PLS component, we quantified the enrichment ratio (defined as the difference between
4 the mean bootstrap weight of the candidate genes and the mean bootstrap weight of the same
5 number of randomly permuted genes), which was then divided by the standard deviation weight
6 of the permuted genes. Significance was determined by percentile of the bootstrap weight of the
7 candidate genes relative to the bootstrap weights of randomly selected genes from 10,000
8 permutations. Positive/negative ER of a given condition indicates that the risk genes are expressed
9 to a higher/lower degree relative to the baseline expression level. In addition, the function of the
10 risk genes needs to be considered when interpreting ER. For example, the FCD candidate genes
11 are inhibitory regulators of mTOR pathway; thus, negative ER for these genes indicates activation
12 of mTOR pathway.

13

14 **Corrections for multiple comparisons**

15 For all spatial correlation analyses, findings were corrected using spin permutation tests at
16 $p_{\text{spin}}=0.05$.⁵⁰ Remaining results were corrected for multiple comparisons using false discovery rate
17 (FDR) at 0.05.⁶⁹

18

19 **Data availability**

20 The data supporting findings of this study are available from the corresponding author upon
21 request. The datasets are not publicly available as they contain information that could compromise
22 privacy of research participants.

23

24

1 Results

2 Cortex-wide MRI distribution of FCD

3 The vertex-wise MRI mapping of FCD lesions across the cortex (**Figure 1**) showed aggregation
4 within the frontal lobe, particularly in prefrontal (dorsolateral, ventrolateral, dorsomedial and
5 medial frontopolar; Brodmann areas 4, 9, 10, 44, 45, 46, 57) and cingulate (anterior-mid and pre-
6 genual; Brodmann areas 24, 32, 33) cortices. The reliability of these areas was supported by higher
7 within-sample and cross-site certainty as compared to the other regions. Lobar mapping also
8 confirmed higher occurrence in the frontal lobe compared to other areas, even after normalizing
9 for lobar surface area.

10

11 Association between FCD distribution and cytoarchitecture

12 With respect to the von Economo and Koskinas data (**Figure 2**), mapping 43 regions per
13 hemisphere, we found a positive correlation between FCD distribution and cortical thickness
14 ($R=0.35$, $p_{spin}<0.05$) and cell size ($R=0.46$, $p_{spin}<0.05$) and a negative correlation with cell density
15 ($R=-0.52$, $p_{spin}<0.001$). We also found a negative correlation with cell density obtained from the
16 BigBrain atlas ($R=-0.34$, $p_{spin}<0.01$). In other words, frontal lobe areas with the highest probability
17 of lesions were those displaying lower neuronal density, larger neurons, and higher cortical
18 thickness.

19

20 Transcriptomic associations and relation to spatiotemporal gene 21 expression

22 Two PLS components explained 25% (PLS-1: $p_{spin}<0.001$) and 27% (PLS-2: $p_{spin}=0.03$) of the
23 covariance between the FCD probability and AHBA gene expression (**Figure 3**). As shown by the
24 gene enrichment analysis, PLS-1 reflected regulation at epigenetic, RNA and post-translational
25 levels, as well as covalent chromatin modification and chromosome organization ($FDR<0.05$),
26 both critical for mitotic cell division and differentiation. Conversely, PLS-2 was mainly

1 characterized by general synaptic organization and activity ($FDR < 0.05$) and marginally by
2 glutamate receptor signaling ($FDR < 0.1$).

3 Evaluating the developmental spatiotemporal trajectories, the expression of genes associated
4 with PLS-1 sharply increased from early to late fetal stages ($FDR < 0.05$), plateaued during infancy
5 and childhood and decreased thereafter ($FDR < 0.05$). Conversely, the expression of genes
6 associated with PLS-2 showed a monotonic increase from early fetal stage to adulthood
7 ($FDR < 0.05$). Expressions were more marked in the frontal lobe, with a fronto-occipital gradient
8 for PLS-1 and a fronto-temporal gradient for PLS-2. We did not find differential associations
9 between early and late onset lesional distribution and the PLS components.

10 **Supplemental Table 1** lists the risk genes used for each condition. Specificity analysis revealed
11 that PLS-1 and PLS-2 were enriched for the risk genes of all epilepsies (PLS-1: $FDR = 0.08$;
12 enrichment ratio, $ER = -2.60$; PLS-2: $FDR < 0.001$, $ER = -3.01$), with PLS-1 additionally enriched for
13 genes causing FCD via somatic mutations ($p < 0.05$, $ER = -1.99$) and risk genes of generalized
14 epilepsy ($FDR = 0.08$, $ER = -2.6$). Neither PLS showed associations to genes for focal epilepsy with
15 hippocampal sclerosis, frontotemporal dementia, bipolar or autism spectrum disorders;
16 **Supplemental Table 2** provides uncorrected p values for the enrichment of the GWAS risk genes.

17

18 **Relation to developmental axes of cortical organization (Figure 4)**

19 The multisite-derived FCD distribution showed a strong positive association with the anterior
20 region of the antero-posterior axis derived from heritability analysis of inter-regional structural
21 covariance of cortical thickness ($R = 0.51$, $p_{spin} < 0.001$), but not with structural ($R = 0.12$, $p = 0.37$)
22 and functional ($R = -0.07$, $p = 0.92$) hierarchical axes.

23

24 **Discussion**

25 We systematically investigated the cellular, genetic and organizational features of cortices
26 harboring FCD. Mapping the cortex-wide MRI distribution of 337 histologically-verified lesions
27 collected from 13 sites worldwide, we found a propensity for the frontal lobe. Associations with

1 histological markers derived from Von Economo and Koskinas and BigBrain atlases showed that
2 in the healthy brain these areas display lower neuronal density, larger neurons and thicker cortices.
3 Using whole-brain and spatiotemporal gene expression datasets, we identified two genetic factors
4 related to FCD distribution: one defined by prenatal regulation of gene expression and
5 chromosome organization and another related to postnatal synapse organization and activity
6 driving neural circuits.⁷⁰ At macroscale, FCD distribution was associated with the antero-posterior
7 organizational axis reflective of the timetable of neurogenesis. Concordant with a causal role of
8 atypical neuroglial proliferation and growth, our results indicate that FCD-vulnerable cortices
9 display cytoarchitectural, molecular and organizational properties indicative of earlier termination
10 of neurogenesis and initiation of cell growth. Our findings also suggest a potential contribution of
11 postnatal synaptogenesis and circuit development to FCD epileptogenicity.

12 While propensity for frontal lobe involvement is in keeping with previous observations,^{1, 9-11}
13 our multisite dataset refined this knowledge by demonstrating locoregional vulnerability of
14 prefrontal and fronto-limbic cortices, the consistency of which was supported by high within-
15 sample and cross-site reliability. Notably, normalizing for lobar surface did not modify results,
16 attesting that such susceptibility is not merely due to the frontal lobe's larger size, but rather linked
17 to intrinsic developmental, likely multifactorial vulnerability. With respect to cytoarchitectural
18 markers, frontal cortices are typified by lower neuronal density, larger cell soma and thicker gray
19 matter. Given that these are also key histopathological traits of FCD,^{2, 71} the association we found
20 may hint at potential pathophysiological developmental processes linked to intrinsic anatomical
21 characteristics of the prefrontal and fronto-limbic cortices. In this context, the timetables of
22 neurogenesis and synaptogenesis of the prefrontal cortices are distinct from other cortices,⁷² as
23 they undergo earlier initiation of proliferation, transition from symmetric (cloning) to asymmetric
24 (differentiation) division, reduction of cell cycle rates and termination of neurogenesis, resulting
25 in lower neuronal density. This is followed by early initiation of neuronal growth leading to larger
26 soma and more complex dendritic arborization of frontal relative to occipital cortices.²⁴⁻²⁶ Hence,
27 although subtle somatic mutations can occur randomly throughout the developing cortex,⁷³ this
28 tighter regulation of neurogenesis in the frontal cortex may explain its heightened susceptibility to
29 harboring FCD. This longer period of cell growth sets the basis for the frontal neurons to undergo
30 a longer period of synaptogenesis,^{72, 74-76} resulting in the overproduction of synapses and a
31 protracted period of pruning.^{74, 75, 77, 78} Similarly, limbic cortices, marked by agranular or

1 dysgranular laminar patterns, develop earlier and undergo longer period of synaptic plasticity
2 through adulthood relative to the isocortex.^{79, 80} Fronto-limbic cortices have shown vulnerability
3 for other developmental disorders, such as schizophrenia^{81, 82} and autism,⁸³⁻⁸⁶ while temporo-
4 limbic cortices preferentially harbor neurodegenerative disorders, namely Alzheimer's and
5 Parkinson's diseases.⁸⁷⁻⁹⁰ Interestingly, tau pathology has been suggested to mediate premature
6 neurodegeneration and cell injury in FCD,^{91, 92} The frontal and limbic regions have been shown to
7 become central hubs in the mature cortical network architecture, which also render themselves
8 vulnerable to structural pathology in numerous lesional and degenerative conditions.^{93, 94}

9 Contextualizing lesional distribution within axes of developmental cortical organization
10 revealed that FCD preferentially occurs in the rostral portion of the anterior-posterior axis defined
11 by genetically determined inter-regional synchrony of cortical development.^{13, 95, 96} Given that this
12 axis reflects the prenatal timetable of neurogenesis and cell growth, the rostral concentration of
13 FCD supports the predisposing roles of aberrant neurogenesis and cell growth as contributors to
14 the histopathological makeup of FCD. In contrast, FCD distribution was disassociated from the
15 sensory-association axis established during late prenatal and postnatal neural circuit
16 development,³¹ a finding consistent with the prenatal occurrence of this malformation.³ A potential
17 genetic underpinning of FCD distribution was also suggested assessing associations to whole-brain
18 gene expression. Indeed, transcriptomic associations based on data-driven PLS regression
19 uncovered a component (PLS-1) reflecting regulation of gene expression at epigenetic, RNA and
20 post-translational levels, as well as covalent chromatin modification and chromosome
21 organization. Chromatin architecture is tightly coupled to mitotic cell cycle and fate. As such, its
22 modification regulated by epigenetic, transcriptional and post-transcriptional mechanisms plays a
23 key role in cell division⁹⁷ and differentiation.⁹⁸ Chromosome organization, which involves
24 assembly, arrangement or disassembly of chromosomes, is the process that allows the parent cell
25 to replicate its DNA such that each daughter cell receives a copy during mitosis.⁹⁹ Therefore,
26 within the cortex, PLS-1 likely represents molecular mechanisms underpinning neuroglial
27 proliferation and differentiation. On the other hand, PLS-2 was related to general synaptic
28 organization and activity, circuit organization,³⁷ as well as glutamate receptor signaling.
29 Evaluating the developmental spatiotemporal trajectories, PLS-1 expression sharply increased
30 from the early fetal stage to late fetal stage, while PLS-2 expression showed steady increase from
31 fetal stages to adulthood. The relevance of these PLS components was supported by the disease

1 specificity analysis. Indeed, while PLS-1 and -2 were both associated with risk genes for all
2 epilepsies, PLS-1 was additionally associated with genes causing FCD via somatic mutations and
3 risk genes of generalized seizures, Therefore, on one hand, it is conceivable that PLS-1 may
4 indicate early cortical vulnerability to aberrant neurogenesis and cell growth, ultimately resulting
5 in a dysplastic lesion. On the other hand, PLS-2 may account for the susceptibility to aberrant
6 synaptogenesis and neurotransmitter systems that for hyperexcitable circuits during a latent period
7 following the precipitating lesion,¹⁰⁰ thereby promoting epileptogenesis. Although synaptic and
8 white matter maturation have been postulated to contribute to FCD occurrence,¹⁰¹ the presented
9 work is the first to provide evidence for the role of postnatal synaptogenesis and circuit
10 development for FCD epileptogenesis.

11
12 Associations with cytoarchitecture, whole-brain and spatiotemporal gene expression, as well as
13 macroscale organizational axes, collectively suggest a vulnerability continuum spanning from
14 prenatal neurogenesis and cell growth to postnatal synaptogenesis. Although age at epilepsy onset
15 has been postulated to account at least partly to variability in FCD histological features,¹⁰² the link
16 to molecular or cellular pathogenic processes remains still unclear. In our study, while we did not
17 find differential associations between early and late disease onset lesional distribution with the
18 PLS components, our findings clearly establish developmental underpinnings of FCD occurrence.
19 To date, a plethora of molecular studies of resected FCD tissues have established a causal role of
20 somatic variants that lead to hyperactivity of the mTOR pathway.^{5, 38, 39, 57, 59, 61, 103-105} A recent
21 large-scale multiomic study of somatic mutations suggested genes implicated in calcium dynamics
22 and synaptic function as potential causes for epileptogenesis.⁸ Nevertheless, given that the variant
23 allelic frequency is typically below 5% in FCD, uncovering variants distinct from mTOR pathway
24 may be difficult, even with a large sample of resected lesions,⁵⁹ Notably, the present study
25 circumvents this logistical and statistical burdens by identifying the genetic fingerprints of the
26 FCD-prone cortices based on noninvasive imaging and offers novel insights that may be difficult
27 to obtain otherwise. It has been shown that somatic activating mutations in the mTOR pathway
28 causes a continuum of malformations, spanning from hemimegalencephaly to posterior
29 quadrantic dysplasia. Although these malformations share some of the genetic determinants with
30 FCD, the time of molecular insult, as well as additional genetic mutations, may lead to varying
31 phenotypes, as suggested by the two-hit germline and somatic mechanisms in

1 hemimegalencephaly.⁵⁷ As for the posterior quadrant dysplasia, prolonged neurogenesis in the
2 posterior isocortex involving higher number and rate of proliferation cycles translates to a greater
3 amplification of abnormal founder cells lesion.¹⁰⁶ Subtle structural, possibly neurodevelopmental
4 anomalies have been reported in generalized genetic epilepsy (GGE) and have been described as
5 microdysgenesis in neuropathological studies^{107, 108} that share histological similarity with FCD
6 Type IA.¹⁰⁹ However, such reports have been sparse, as GGE patients generally do not undergo
7 surgery. Furthermore, the replicability of identifying microdysgenesis in GGE has been limited,
8 thereby not establishing it as a common feature of this condition.¹¹⁰ In terms of genotype-
9 phenotype associations, while the cellular mechanisms that drive the histopathological features of
10 dysplasia are being elucidated,⁷ those underlying circuit-level alterations that drive recurrent
11 seizures in this condition remain elusive. Conceivably, mitigating the circuit-level alterations
12 precipitated by FCD may reduce seizures.¹⁰⁰ Hence, future work should elucidate the molecular
13 and cellular mechanisms of aberrant postnatal synaptogenesis that drive circuit hyperexcitability
14 and identify novel therapeutic targets, possibly combined with mTOR inhibitors, for improved
15 seizure control.

16

17 **Funding**

18 This work was supported by the Canadian Institutes of Health Research to A.B. and N.B. (MOP-
19 57840 and 123520), Natural Sciences and Engineering Research Council of Canada
20 (Discovery-243141 to AB and 24779 to N.B.), Epilepsy Canada (Jay & Aiden Barker
21 Breakthrough Grant in Clinical & Basic Sciences to A.B.), and Brain Canada. Salary supports
22 were provided by Fonds de Recherche Sante – Quebec, Savoy Foundation for Epilepsy (H.-M.L.),
23 and Lloyd Carr-Harris Foundation (B.C.).

24

25 **Competing interests**

26 The authors declare that they have no known competing financial interests or personal
27 relationships that could have appeared to influence the work reported in this paper.

28

1 **Supplementary material**

2 Supplementary material is available at *Brain* online.

3

4 **References**

- 5 1. Blumcke I, Spreafico R, Haaker G, et al. Histopathological Findings in Brain Tissue
6 Obtained during Epilepsy Surgery. *New England Journal of Medicine*. 2017/10/26
7 2017;377(17):1648-1656. doi:10.1056/NEJMoa1703784
- 8 2. Blumcke I, Thom M, Aronica E, et al. The clinicopathologic spectrum of focal cortical
9 dysplasias: a consensus classification proposed by an ad hoc Task Force of the ILAE Diagnostic
10 Methods Commission. *Epilepsia*. Jan 2011;52(1):158-74. doi:10.1111/j.1528-1167.2010.02777.x
- 11 3. Iffland PH, Crino PB. Focal Cortical Dysplasia: Gene Mutations, Cell Signaling, and
12 Therapeutic Implications. *Annual Review of Pathology: Mechanisms of Disease*. 2017/01/24
13 2017;12(1):547-571. doi:10.1146/annurev-pathol-052016-100138
- 14 4. Jamuar SS, Lam A-TN, Kircher M, et al. Somatic Mutations in Cerebral Cortical
15 Malformations. *New England Journal of Medicine*. 2014/08/21 2014;371(8):733-743.
16 doi:10.1056/NEJMoa1314432
- 17 5. Lim JS, Kim W-i, Kang H-C, et al. Brain somatic mutations in MTOR cause focal cortical
18 dysplasia type II leading to intractable epilepsy. *Nature Medicine*. 03/23/online 2015;21:395.
19 doi:10.1038/nm.3824
20 <https://www.nature.com/articles/nm.3824#supplementary-information>
- 21 6. D'Gama AM, Geng Y, Couto JA, et al. Mammalian target of rapamycin pathway mutations
22 cause hemimegalencephaly and focal cortical dysplasia. *Annals of neurology*. 2015;77(4):720-725.
23 doi:10.1002/ana.24357
- 24 7. Park SM, Lim JS, Ramakrishna S, et al. Brain Somatic Mutations in MTOR Disrupt
25 Neuronal Ciliogenesis, Leading to Focal Cortical Dyslamination. *Neuron*. 2018/07/11/
26 2018;99(1):83-97.e7. doi:<https://doi.org/10.1016/j.neuron.2018.05.039>

- 1 8. Chung C, Yang X, Bae T, et al. Comprehensive multiomic profiling of somatic mutations
2 in malformations of cortical development. *bioRxiv*. 2022:2022.04.07.487401.
3 doi:10.1101/2022.04.07.487401
- 4 9. Lamberink HJ, Otte WM, Blümcke I, et al. Seizure outcome and use of antiepileptic drugs
5 after epilepsy surgery according to histopathological diagnosis: a retrospective multicentre cohort
6 study. *The Lancet Neurology*. 2020;19(9):748-757. doi:10.1016/S1474-4422(20)30220-9
- 7 10. Gill RS, Lee H-M, Caldaïrou B, et al. Multicenter validation of a deep learning detection
8 algorithm for focal cortical dysplasia. *Neurology*. 2021;97(16):e1571-e1582.
- 9 11. Wagstyl K, Whitaker K, Raznahan A, et al. Atlas of lesion locations and postsurgical
10 seizure freedom in focal cortical dysplasia: A MELD study. *Epilepsia*. 2021;
- 11 12. Cadwell CR, Bhaduri A, Mostajo-Radji MA, Keefe MG, Nowakowski TJ. Development
12 and arealization of the cerebral cortex. *Neuron*. 2019;103(6):980-1004.
- 13 13. Valk SL, Xu T, Margulies DS, et al. Shaping brain structure: Genetic and phylogenetic
14 axes of macroscale organization of cortical thickness. *Science advances*. 2020;6(39):eabb3417.
- 15 14. Klingler E, Francis F, Jabaudon D, Cappello S. Mapping the molecular and cellular
16 complexity of cortical malformations. *Science*. 2021;371(6527)
- 17 15. Hawrylycz M, Miller JA, Menon V, et al. Canonical genetic signatures of the adult human
18 brain. *Nature Neuroscience*. 2015/12/01 2015;18(12):1832-1844. doi:10.1038/nn.4171
- 19 16. Silbereis JC, Pochareddy S, Zhu Y, Li M, Sestan N. The cellular and molecular landscapes
20 of the developing human central nervous system. *Neuron*. 2016;89(2):248-268.
- 21 17. Burt JB, Demirtaş M, Eckner WJ, et al. Hierarchy of transcriptomic specialization across
22 human cortex captured by structural neuroimaging topography. *Nature neuroscience*.
23 2018;21(9):1251-1259.
- 24 18. Paquola C, Benkarim O, DeKraker J, et al. Convergence of cortical types and functional
25 motifs in the human mesiotemporal lobe. *Elife*. 2020;9:e60673.
- 26 19. Demirtaş M, Burt JB, Helmer M, et al. Hierarchical heterogeneity across human cortex
27 shapes large-scale neural dynamics. *Neuron*. 2019;101(6):1181-1194. e13.

- 1 20. Wagstyl K, Ronan L, Goodyer IM, Fletcher PC. Cortical thickness gradients in structural
2 hierarchies. *Neuroimage*. 2015;111:241-250.
- 3 21. Huntenburg JM, Bazin P-L, Margulies DS. Large-Scale Gradients in Human Cortical
4 Organization. *Trends in Cognitive Sciences*. 2018/01/01/ 2018;22(1):21-31.
5 doi:<https://doi.org/10.1016/j.tics.2017.11.002>
- 6 22. Park B-y, de Wael RV, Paquola C, et al. Signal diffusion along connectome gradients and
7 inter-hub routing differentially contribute to dynamic human brain function. *NeuroImage*.
8 2021;224:117429.
- 9 23. Margulies DS, Ghosh SS, Goulas A, et al. Situating the default-mode network along a
10 principal gradient of macroscale cortical organization. *Proceedings of the National Academy of*
11 *Sciences*. 2016;113(44):12574-12579. doi:10.1073/pnas.1608282113
- 12 24. Chen C-H, Panizzon MS, Eyer LT, et al. Genetic influences on cortical regionalization in
13 the human brain. *Neuron*. 2011;72(4):537-544.
- 14 25. Cahalane DJ, Charvet CJ, Finlay BL. Systematic, balancing gradients in neuron density
15 and number across the primate isocortex. *Front Neuroanat*. 2012;6:28-28.
16 doi:10.3389/fnana.2012.00028
- 17 26. Charvet CJ, Finlay BL. Evo-devo and the primate isocortex: the central organizing role of
18 intrinsic gradients of neurogenesis. *Brain, behavior and evolution*. 2014;84(2):81-92.
- 19 27. Paquola C, Royer J, Lewis LB, et al. The BigBrainWarp toolbox for integration of
20 BigBrain 3D histology with multimodal neuroimaging. *eLife*. 2021/08/25 2021;10:e70119.
21 doi:10.7554/eLife.70119
- 22 28. Paquola C, Vos De Wael R, Wagstyl K, et al. Microstructural and functional gradients are
23 increasingly dissociated in transmodal cortices. *PLOS Biology*. 2019;17(5):e3000284.
24 doi:10.1371/journal.pbio.3000284
- 25 29. Sydnor VJ, Larsen B, Bassett DS, et al. Neurodevelopment of the association cortices:
26 Patterns, mechanisms, and implications for psychopathology. *Neuron*. 2021;
- 27 30. Mesulam MM. From sensation to cognition. *Brain*. 1998;121(6):1013-1052.
28 doi:10.1093/brain/121.6.1013

- 1 31. Price DJ, Kennedy H, Dehay C, et al. The development of cortical connections. *European*
2 *Journal of Neuroscience*. 2006;23(4):910-920. doi:[https://doi.org/10.1111/j.1460-](https://doi.org/10.1111/j.1460-9568.2006.04620.x)
3 [9568.2006.04620.x](https://doi.org/10.1111/j.1460-9568.2006.04620.x)
- 4 32. von Economo CF, Koskinas GN. *Die cytoarchitektonik der hirnrinde des erwachsenen*
5 *menschen*. J. Springer; 1925.
- 6 33. Scholtens LH, de Reus MA, de Lange SC, Schmidt R, van den Heuvel MP. An mri von
7 economo–koskinas atlas. *Neuroimage*. 2018;170:249-256.
- 8 34. Amunts K, Lepage C, Borgeat L, et al. BigBrain: An Ultrahigh-Resolution 3D Human
9 Brain Model. *Science*. 2013;340(6139):1472-1475. doi:doi:10.1126/science.1235381
- 10 35. Hawrylycz MJ, Lein ES, Guillozet-Bongaarts AL, et al. An anatomically comprehensive
11 atlas of the adult human brain transcriptome. *Nature*. 2012;489(7416):391-399.
- 12 36. Li M, Santpere G, Imamura Kawasawa Y, et al. Integrative functional genomic analysis of
13 human brain development and neuropsychiatric risks. *Science*. 2018;362(6420):eaat7615.
14 doi:10.1126/science.aat7615
- 15 37. Zhu Y, Sousa AMM, Gao T, et al. Spatiotemporal transcriptomic divergence across human
16 and macaque brain development. *Science*. 2018;362(6420):eaat8077. doi:10.1126/science.aat8077
- 17 38. Marsan E, Baulac S. Review: Mechanistic target of rapamycin (mTOR) pathway, focal
18 cortical dysplasia and epilepsy. *Neuropathology and Applied Neurobiology*. 2018/02/01
19 2018;44(1):6-17. doi:10.1111/nan.12463
- 20 39. Avansini SH, Torres FR, Vieira AS, et al. Dysregulation of NEUROG2 plays a key role in
21 focal cortical dysplasia. *Annals of Neurology*. 2018;83(3):623-635.
22 doi:<https://doi.org/10.1002/ana.25187>
- 23 40. Consortium TILAE. Genome-wide mega-analysis identifies 16 loci and highlights diverse
24 biological mechanisms in the common epilepsies. *Nature communications*. 2018;9
- 25 41. Bernasconi A, Cendes F, Theodore WH, et al. Recommendations for the use of structural
26 magnetic resonance imaging in the care of patients with epilepsy: a consensus report from the
27 International League Against Epilepsy Neuroimaging Task Force. *Epilepsia*. 2019;60(6):1054-
28 1068.

- 1 42. Kim JS, Singh V, Lee JK, et al. Automated 3-D extraction and evaluation of the inner and
2 outer cortical surfaces using a Laplacian map and partial volume effect classification. *NeuroImage*.
3 2005/08/01/ 2005;27(1):210-221. doi:<https://doi.org/10.1016/j.neuroimage.2005.03.036>
- 4 43. Lyttelton O, Boucher M, Robbins S, Evans A. An unbiased iterative group registration
5 template for cortical surface analysis. *Neuroimage*. 2007;34(4):1535-1544.
- 6 44. Hong S-J, Bernhardt BC, Caldirou B, et al. Multimodal MRI profiling of focal cortical
7 dysplasia type II. *Neurology*. January 27, 2017 2017;88:734-742.
8 doi:10.1212/WNL.0000000000003632
- 9 45. Tzourio-Mazoyer N, Landeau B, Papathanassiou D, et al. Automated Anatomical Labeling
10 of Activations in SPM Using a Macroscopic Anatomical Parcellation of the MNI MRI Single-
11 Subject Brain. *NeuroImage*. 2002/01/01/ 2002;15(1):273-289.
12 doi:<https://doi.org/10.1006/nimg.2001.0978>
- 13 46. Schaefer A, Kong R, Gordon EM, et al. Local-Global Parcellation of the Human Cerebral
14 Cortex from Intrinsic Functional Connectivity MRI. *Cereb Cortex*. Sep 1 2018;28(9):3095-3114.
15 doi:10.1093/cercor/bhx179
- 16 47. Desikan RS, Ségonne F, Fischl B, et al. An automated labeling system for subdividing the
17 human cerebral cortex on MRI scans into gyral based regions of interest. *Neuroimage*.
18 2006;31(3):968-980.
- 19 48. Whitaker KJ, Vértes PE, Romero-Garcia R, et al. Adolescence is associated with
20 genomically patterned consolidation of the hubs of the human brain connectome. *Proceedings of*
21 *the National Academy of Sciences*. 2016;113(32):9105. doi:10.1073/pnas.1601745113
- 22 49. de Wael RV, Benkarim O, Paquola C, et al. BrainSpace: a toolbox for the analysis of
23 macroscale gradients in neuroimaging and connectomics datasets. *Communications biology*.
24 2020;3(1):1-10.
- 25 50. Alexander-Bloch AF, Shou H, Liu S, et al. On testing for spatial correspondence between
26 maps of human brain structure and function. *NeuroImage*. 2018/09/01/ 2018;178:540-551.
27 doi:<https://doi.org/10.1016/j.neuroimage.2018.05.070>

- 1 51. Liao Y, Wang J, Jaehnig EJ, Shi Z, Zhang B. WebGestalt 2019: gene set analysis toolkit
2 with revamped UIs and APIs. *Nucleic Acids Research*. 2019;47(W1):W199-W205.
3 doi:10.1093/nar/gkz401
- 4 52. Kang HJ, Kawasaki YI, Cheng F, et al. Spatio-temporal transcriptome of the human brain.
5 *Nature*. 2011/10/01 2011;478(7370):483-489. doi:10.1038/nature10523
- 6 53. Jansen LA, Mirzaa GM, Ishak GE, et al. PI3K/AKT pathway mutations cause a spectrum
7 of brain malformations from megalencephaly to focal cortical dysplasia. *Brain*. 2015;138(6):1613-
8 1628.
- 9 54. Terrone G, Voisin N, Alfaiz AA, et al. De novo PIK3R2 variant causes polymicrogyria,
10 corpus callosum hyperplasia and focal cortical dysplasia. *European Journal of Human Genetics*.
11 2016;24(9):1359-1362.
- 12 55. Kobow K, Ziemann M, Kaipananickal H, et al. Genomic DNA methylation distinguishes
13 subtypes of human focal cortical dysplasia. *Epilepsia*. 2019;60(6):1091-1103.
- 14 56. Schick V, Majores M, Engels G, et al. Activation of Akt independent of PTEN and CTMP
15 tumor-suppressor gene mutations in epilepsy-associated Taylor-type focal cortical dysplasias. *Acta*
16 *neuropathologica*. 2006;112(6):715-725.
- 17 57. D’Gama AM, Woodworth MB, Hossain AA, et al. Somatic mutations activating the mTOR
18 pathway in dorsal telencephalic progenitors cause a continuum of cortical dysplasias. *Cell reports*.
19 2017;21(13):3754-3766.
- 20 58. Lim JS, Gopalappa R, Kim SH, et al. Somatic mutations in TSC1 and TSC2 cause focal
21 cortical dysplasia. *The American Journal of Human Genetics*. 2017;100(3):454-472.
- 22 59. Baldassari S, Ribierre T, Marsan E, et al. Dissecting the genetic basis of focal cortical
23 dysplasia: a large cohort study. *Acta neuropathologica*. 2019;138(6):885-900.
- 24 60. Sim JC, Scerri T, Fanjul-Fernández M, et al. Familial cortical dysplasia caused by mutation
25 in the mammalian target of rapamycin regulator NPRL3. *Annals of neurology*. 2016;79(1):132-
26 137.
- 27 61. Zhang Z, Gao K, Liu Q, et al. Somatic variants in new candidate genes identified in focal
28 cortical dysplasia type II. *Epilepsia*. 2020;61(4):667-678.

- 1 62. Baulac S, Ishida S, Marsan E, et al. Familial focal epilepsy with focal cortical dysplasia
2 due to DEPDC 5 mutations. *Annals of neurology*. 2015;77(4):675-683.
- 3 63. Carvill GL, Crompton DE, Regan BM, et al. Epileptic spasms are a feature of DEPDC5
4 mTORopathy. *Neurology Genetics*. 2015;1(2)
- 5 64. Scerri T, Riseley JR, Gillies G, et al. Familial cortical dysplasia type IIA caused by a
6 germline mutation in DEPDC 5. *Annals of clinical and translational neurology*. 2015;2(5):575-
7 580.
- 8 65. Ying Z, Wang I, Blümcke I, et al. A comprehensive clinico-pathological and genetic
9 evaluation of bottom-of-sulcus focal cortical dysplasia in patients with difficult-to-localize focal
10 epilepsy. *Epileptic Disorders*. 2019;21(1):65-77.
- 11 66. Grove J, Ripke S, Als TD, et al. Identification of common genetic risk variants for autism
12 spectrum disorder. *Nat Genet*. 2019;51(3):431-444.
- 13 67. Stahl EA, Breen G, Forstner AJ, et al. Genome-wide association study identifies 30 loci
14 associated with bipolar disorder. *Nat Genet*. 2019;51(5):793-803.
- 15 68. Ferrari R, Hernandez DG, Nalls MA, et al. Frontotemporal dementia and its subtypes: a
16 genome-wide association study. *The Lancet Neurology*. 2014;13(7):686-699. doi:10.1016/S1474-
17 4422(14)70065-1
- 18 69. Benjamini Y, Hochberg Y. Controlling the False Discovery Rate: A Practical and Powerful
19 Approach to Multiple Testing. *Journal of the Royal Statistical Society Series B (Methodological)*.
20 1995;57(1):289-300.
- 21 70. Katz LC, Shatz CJ. Synaptic activity and the construction of cortical circuits. *Science*.
22 1996;274(5290):1133-1138.
- 23 71. Thom M, Martinian L, Sen A, Cross JH, Harding BN, Sisodiya SM. Cortical neuronal
24 densities and lamination in focal cortical dysplasia. *Acta Neuropathologica*. 2005/10/01
25 2005;110(4):383-392. doi:10.1007/s00401-005-1062-0
- 26 72. Kolk SM, Rakic P. Development of prefrontal cortex. *Neuropsychopharmacology*.
27 2022;47(1):41-57.

- 1 73. Wang Y, Bae T, Thorpe J, et al. Comprehensive identification of somatic nucleotide
2 variants in human brain tissue. *Genome Biology*. 2021/03/29 2021;22(1):92. doi:10.1186/s13059-
3 021-02285-3
- 4 74. Kroon T, van Hugte E, van Linge L, Mansvelder HD, Meredith RM. Early postnatal
5 development of pyramidal neurons across layers of the mouse medial prefrontal cortex. *Scientific*
6 *Reports*. 2019/03/25 2019;9(1):5037. doi:10.1038/s41598-019-41661-9
- 7 75. Huttenlocher PR, Dabholkar AS. Regional differences in synaptogenesis in human cerebral
8 cortex. *Journal of comparative Neurology*. 1997;387(2):167-178.
- 9 76. Lenroot RK, Giedd JN. Brain development in children and adolescents: insights from
10 anatomical magnetic resonance imaging. *Neuroscience & biobehavioral reviews*. 2006;30(6):718-
11 729.
- 12 77. Petanjek Z, Judaš M, Šimić G, et al. Extraordinary neoteny of synaptic spines in the human
13 prefrontal cortex. *Proceedings of the National Academy of Sciences*. 2011;108(32):13281-13286.
- 14 78. Mrzljak L, Uylings HB, Kostovic I, van Eden CG. Prenatal development of neurons in the
15 human prefrontal cortex: I. A qualitative Golgi study. *Journal of comparative neurology*.
16 1988;271(3):355-386.
- 17 79. García-Cabezas MÁ, Zikopoulos B, Barbas H. The Structural Model: a theory linking
18 connections, plasticity, pathology, development and evolution of the cerebral cortex. *Brain*
19 *Structure and Function*. 2019;224(3):985-1008.
- 20 80. Barbas H. General Cortical and Special Prefrontal Connections: Principles from Structure
21 to Function. *Annual Review of Neuroscience*. 2015;38(1):269-289. doi:10.1146/annurev-neuro-
22 071714-033936
- 23 81. Benes FM, Vincent SL, Todtenkopf M. The density of pyramidal and nonpyramidal
24 neurons in anterior cingulate cortex of schizophrenic and bipolar subjects. *Biological psychiatry*.
25 2001;50(6):395-406.
- 26 82. Park B-y, Kebets V, Larivière S, et al. Multilevel neural gradients reflect transdiagnostic
27 effects of major psychiatric conditions on cortical morphology. *bioRxiv*. 2021:2021.10.29.466434.
28 doi:10.1101/2021.10.29.466434

- 1 83. Zikopoulos B, Barbas H. Changes in prefrontal axons may disrupt the network in autism.
2 *Journal of Neuroscience*. 2010;30(44):14595-14609.
- 3 84. Wegiel J, Kuchna I, Nowicki K, et al. The neuropathology of autism: defects of
4 neurogenesis and neuronal migration, and dysplastic changes. *Acta neuropathologica*.
5 2010;119(6):755-770.
- 6 85. Casanova MF, El-Baz AS, Kamat SS, et al. Focal cortical dysplasias in autism spectrum
7 disorders. *Acta neuropathologica communications*. 2013;1(1):1-11.
- 8 86. Valk SL, Di Martino A, Milham MP, Bernhardt BC. Multicenter mapping of structural
9 network alterations in autism. *Human Brain Mapping*. 2015;36(6):2364-2373.
10 doi:<https://doi.org/10.1002/hbm.22776>
- 11 87. Arnold SE, Hyman BT, Flory J, Damasio AR, Van Hoesen GW. The topographical and
12 neuroanatomical distribution of neurofibrillary tangles and neuritic plaques in the cerebral cortex
13 of patients with Alzheimer's disease. *Cerebral cortex*. 1991;1(1):103-116.
- 14 88. Duyckaerts C, CoLLE M-A, Dessi F, Piette F, Hauw J. Progression of Alzheimer
15 histopathological changes. *Acta neurologica belgica*. 1998;98:180-185.
- 16 89. Braak H, Del Tredici K. Spreading of tau pathology in sporadic Alzheimer's disease along
17 cortico-cortical top-down connections. *Cerebral Cortex*. 2018;28(9):3372-3384.
- 18 90. Brettschneider J, Tredici KD, Lee VM-Y, Trojanowski JQ. Spreading of pathology in
19 neurodegenerative diseases: a focus on human studies. *Nature Reviews Neuroscience*.
20 2015;16(2):109-120.
- 21 91. Sen A, Thom M, Martinian L, et al. Pathological Tau Tangles Localize to Focal Cortical
22 Dysplasia in Older Patients. *Epilepsia*. 2007;48(8):1447-1454. doi:[https://doi.org/10.1111/j.1528-
23 1167.2007.01107.x](https://doi.org/10.1111/j.1528-1167.2007.01107.x)
- 24 92. Iyer A, Prabowo A, Anink J, Spliet WGM, van Rijen PC, Aronica E. Cell injury and
25 Premature Neurodegeneration in Focal Malformations of Cortical Development. *Brain Pathology*.
26 2014;24(1):1-17. doi:<https://doi.org/10.1111/bpa.12060>
- 27 93. Crossley NA, Mechelli A, Scott J, et al. The hubs of the human connectome are generally
28 implicated in the anatomy of brain disorders. *Brain*. 2014;137(8):2382-2395.

- 1 94. Sporns O. Towards network substrates of brain disorders. *Brain*. 2014;137(8):2117-2118.
- 2 95. Raznahan A, Lerch Jason P, Lee N, et al. Patterns of Coordinated Anatomical Change in
3 Human Cortical Development: A Longitudinal Neuroimaging Study of Maturational Coupling.
4 *Neuron*. 2011/12/08/ 2011;72(5):873-884. doi:<https://doi.org/10.1016/j.neuron.2011.09.028>
- 5 96. Alexander-Bloch A, Raznahan A, Bullmore E, Giedd J. The Convergence of Maturational
6 Change and Structural Covariance in Human Cortical Networks. *The Journal of Neuroscience*.
7 2013;33(7):2889-2899. doi:10.1523/jneurosci.3554-12.2013
- 8 97. Ma Y, Kanakousaki K, Buttitta L. How the cell cycle impacts chromatin architecture and
9 influences cell fate. Review. *Frontiers in Genetics*. 2015-February-03
10 2015;6doi:10.3389/fgene.2015.00019
- 11 98. Bernstein BE, Mikkelsen TS, Xie X, et al. A Bivalent Chromatin Structure Marks Key
12 Developmental Genes in Embryonic Stem Cells. *Cell*. 2006;125(2):315-326.
13 doi:10.1016/j.cell.2006.02.041
- 14 99. Batty P, Gerlich DW. Mitotic Chromosome Mechanics: How Cells Segregate Their
15 Genome. *Trends in Cell Biology*. 2019;29(9):717-726. doi:10.1016/j.tcb.2019.05.007
- 16 100. Goldberg EM, Coulter DA. Mechanisms of epileptogenesis: a convergence on neural
17 circuit dysfunction. *Nature Reviews Neuroscience*. 2013;14(5):337-349.
- 18 101. Cohen NT, You X, Krishnamurthy M, et al. Networks Underlie Temporal Onset of
19 Dysplasia-Related Epilepsy: A MELD Study. *Annals of Neurology*. 2022;92(3):503-511.
20 doi:<https://doi.org/10.1002/ana.26442>
- 21 102. Fauser S, Huppertz H-J, Bast T, et al. Clinical characteristics in focal cortical dysplasia: a
22 retrospective evaluation in a series of 120 patients. *Brain*. 2006;129(7):1907-1916.
23 doi:10.1093/brain/awl133
- 24 103. Møller RS, Weckhuysen S, Chipaux M, et al. Germline and somatic mutations in the
25 MTOR gene in focal cortical dysplasia and epilepsy. *Neurology Genetics*. 2016;2(6):e118-e118.
26 doi:10.1212/NXG.0000000000000118

- 1 104. Nakashima M, Saitsu H, Takei N, et al. Somatic Mutations in the MTOR gene cause focal
2 cortical dysplasia type IIb. *Annals of Neurology*. 2015/09/01 2015;78(3):375-386.
3 doi:10.1002/ana.24444
- 4 105. Zhao S, Li Z, Zhang M, et al. A brain somatic RHEB doublet mutation causes focal cortical
5 dysplasia type II. *Experimental & Molecular Medicine*. 2019/07/01 2019;51(7):1-11.
6 doi:10.1038/s12276-019-0277-4
- 7 106. D'Agostino MD, Bastos A, Piras C, et al. Posterior quadrantic dysplasia or hemi-
8 hemimegalencephaly. *A characteristic brain malformation*. 2004;62(12):2214-2220.
9 doi:10.1212/01.Wnl.0000130459.91445.91
- 10 107. Kasper BS, Chang BS, Kasper EM. Microdysgenesis: Historical roots of an important
11 concept in epilepsy. *Epilepsy & Behavior*. 2009/06/01/ 2009;15(2):146-153.
12 doi:<https://doi.org/10.1016/j.yebeh.2009.03.026>
- 13 108. Najm I, Lal D, Alonso Vanegas M, et al. The ILAE consensus classification of focal
14 cortical dysplasia: An update proposed by an ad hoc task force of the ILAE diagnostic methods
15 commission. *Epilepsia*. 2022;63(8):1899-1919.
- 16 109. Palmini A, Najm I, Avanzini G, et al. Terminology and classification of the cortical
17 dysplasias. *Neurology*. 2004;62(6 suppl 3):S2-S8. doi:10.1212/01.Wnl.0000114507.30388.7e
- 18 110. Opeskin K, Kalnins RM, Halliday G, Cartwright H, Berkovic SF. Idiopathic generalized
19 epilepsy. *Lack of significant microdysgenesis*. 2000;55(8):1101-1106. doi:10.1212/wnl.55.8.1101

20
21

1 **Figure legends**

2
3 **Figure 1 Cortex-wide FCD distribution.** **A.** For each patient, the FCD lesion was manually
4 segmented on MRI and mapped onto its cortical surface. **B.** Map of FCD distribution. **C.**
5 Reliability analysis. Within-sample and cross-site robustness of regional FCD probability is high
6 where the FCD probability is high. **D.** Lobar distribution. The spider plot of the FCD distribution
7 across lobes demonstrates remarkable preference towards the frontal lobe, which holds after
8 normalizing for the surface area of each lobe (dotted line).

9
10 **Figure 2 Associations between FCD distribution and histological measures.** Plots show
11 correlations between FCD probability and cortical thickness, cell size, and cell density derived
12 from the Von Economo-Koskinas atlas (**A**), as well as cell density (in arbitrary units, a.u.) indexed
13 by optical density of silver-stained cells in the BigBrain atlas (**B**). In the scatterplots, x- and y-axes
14 represent FCD probability (in %) and histological quantities, respectively; dots indicate 308
15 parcels of the Desikan-Killiany atlas. Color-coding is identical for brain maps and dots; p_{spin}
16 indicates p value after adjusting for spatial autocorrelation.

17
18 **Figure 3 Cortex-wide association between FCD topography and gene expression.** **A.** Partial
19 least squares (PLS) regression identified weighted combinations of genes, or PLS components,
20 and their spatial expression profiles that best explained the regional variance in FCD distribution,
21 or percent variance explained; p_{spin} indicates p value after adjusting for spatial autocorrelation).
22 Inputs to PLS include the whole-brain gene expression data matrix (parcels by genes) and FCD
23 distribution across parcels (in %). Outputs include gene weights (genes by components), gene
24 spatial profiles (parcels by components) and percent variance explained by PLS components. **B.**
25 Maps of gene expression. The color scale indicates the score for PLS-1 and 2, namely the weighted
26 average expression level of 20,737. **C.** Gene enrichment analysis. Genes associated with PLS-1
27 were enriched for epigenetic, RNA and post-translational levels as well as covalent chromatin
28 modification and chromosome organization; and PLS-2 for general synapse organization and
29 activity. In the volcano plots, x-axis indicates \log_2 of enrichment ratio and y-axis indicates $-\log_{10}$

1 of FDR. Color codes indicate the number of genes related to the biological processes that overlap
2 with the input list of top 10 percentile genes; upper/lower dotted lines indicate FDR=0.05/0.1. **D.**
3 Developmental spatiotemporal trajectory. The expression of genes associated with PLS-1 sharply
4 increased from early to late fetal stages, plateaued during infancy and childhood, and decreased
5 thereafter. Conversely, PLS-2 showed monotonic increase from early fetal stage to adulthood. In
6 both instances, expressions were more marked in the frontal lobe. Dots represent cortical samples
7 at a given timepoint color-coded by lobes; dotted lines connecting dots correspond to the same
8 region of interest. Thick colored lines connect the average of samples within each time window,
9 thereby showing the overall trajectory. Asterisks indicate FDR<0.05. **E.** Specificity analysis. PLS-
10 1 was significantly enriched for FCD pathogenic genes; the histogram shows bootstrap weights of
11 10,000 permutations; the dotted line indicates the bootstrap weight of the candidate genes. In
12 relation to GWAS-risk genes, PLS-2 (blue) was enriched for genes associated with all epilepsies,
13 while PLS-1 (red) was marginally enriched for those associated with all and generalized epilepsies.
14 Top dotted line indicates FDR = 0.05; bottom dotted line indicates FDR = 0.1.

15
16 **Figure 4 Relation to developmental axes of cortical organization.** FCD distribution showed a
17 strong association with the anterior region of the antero-posterior axis derived from heritability
18 analysis of inter-regional structural covariance of cortical thickness (**A**), but not with structural (**B**)
19 and functional (**C**) hierarchical axes. X and y- axes represent the FCD probability (in %) and the
20 rank along the gradient axes, also represented as maps. The color scale represents the percentage
21 of patients in whom the FCD is located at a given vertex.

22
23

1 **Table I Site-specific demographics**

2

	Sample size (n)	FCD IIA/IIB	Age (years)	Sex (female/male)	Age at onset (years)
All	337	134/203	22.2 ± 12.7	153/184	7.6 ± 6.7
S1	114	55/59	24.8 ± 10.5	56/58	9.1 ± 7.1
S2	8	3/5	10.5 ± 6.4	2/6	5.5 ± 4.2
S3	10	2/8	25.3 ± 14.2	5/5	7.2 ± 7.4
S4	43	6/37	24.3 ± 14.4	20/23	7.3 ± 7.6
S5	18	9/9	6.8 ± 5.6	8/10	5.6 ± 4.1
S6	22	13/9	17.4 ± 13.5	8/14	5.0 ± 4.8
S7	11	4/7	30.8 ± 14.0	7/4	4.1 ± 3.1
S8	14	3/11	29.1 ± 11.8	5/9	7.5 ± 5.6
S9	8	0/8	31.9 ± 15.3	3/5	8.9 ± 4.7
S10	14	7/7	25.3 ± 7.5	6/8	9.9 ± 5.6
S11	11	6/5	20.8 ± 6.8	7/4	6.8 ± 8.2
S12	42	17/25	17.0 ± 10.7	17/25	6.6 ± 5.8
S13	22	9/13	20.9 ± 15.5	9/13	7.1 ± 8.6

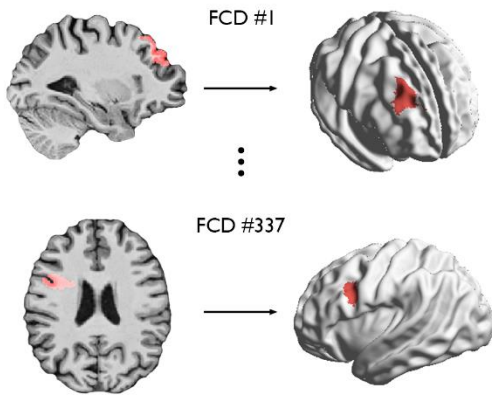
3 Data for age and age at onset indicate mean ± standard deviation.

4

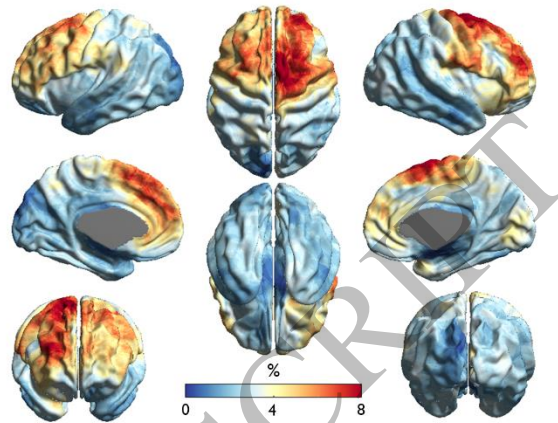
5

ACCEPTED MANUSCRIPT

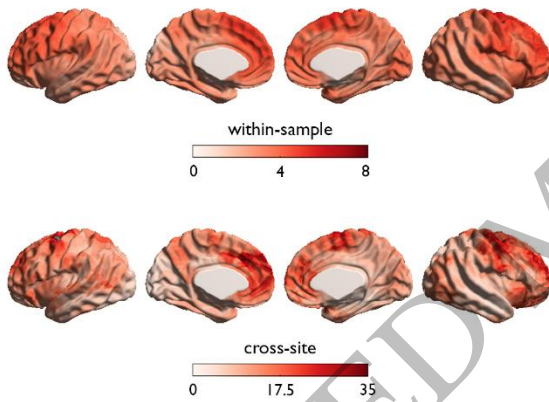
A FCD segmentation and surface projection



B Map of FCD distribution



C Reliability analysis



D Lobar distribution

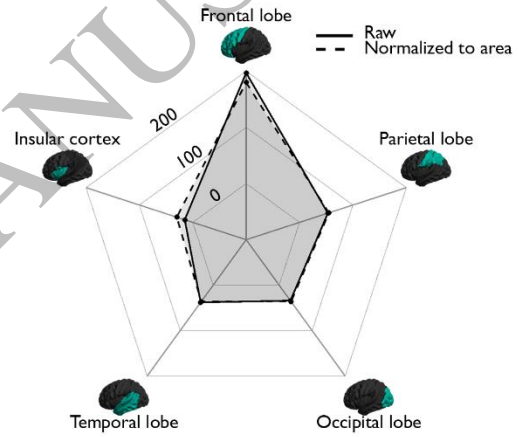
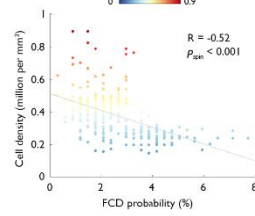
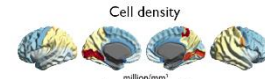
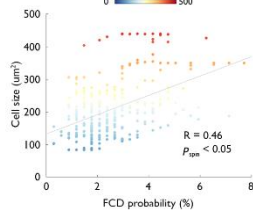
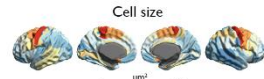
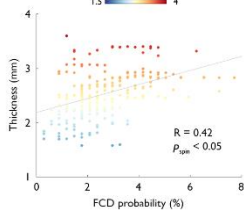


Figure 1
159x135 mm (x DPI)

1
2
3
4

A Von Economo - Koskinas atlas



B BigBrain atlas

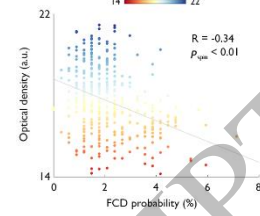
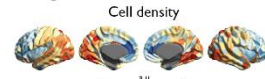
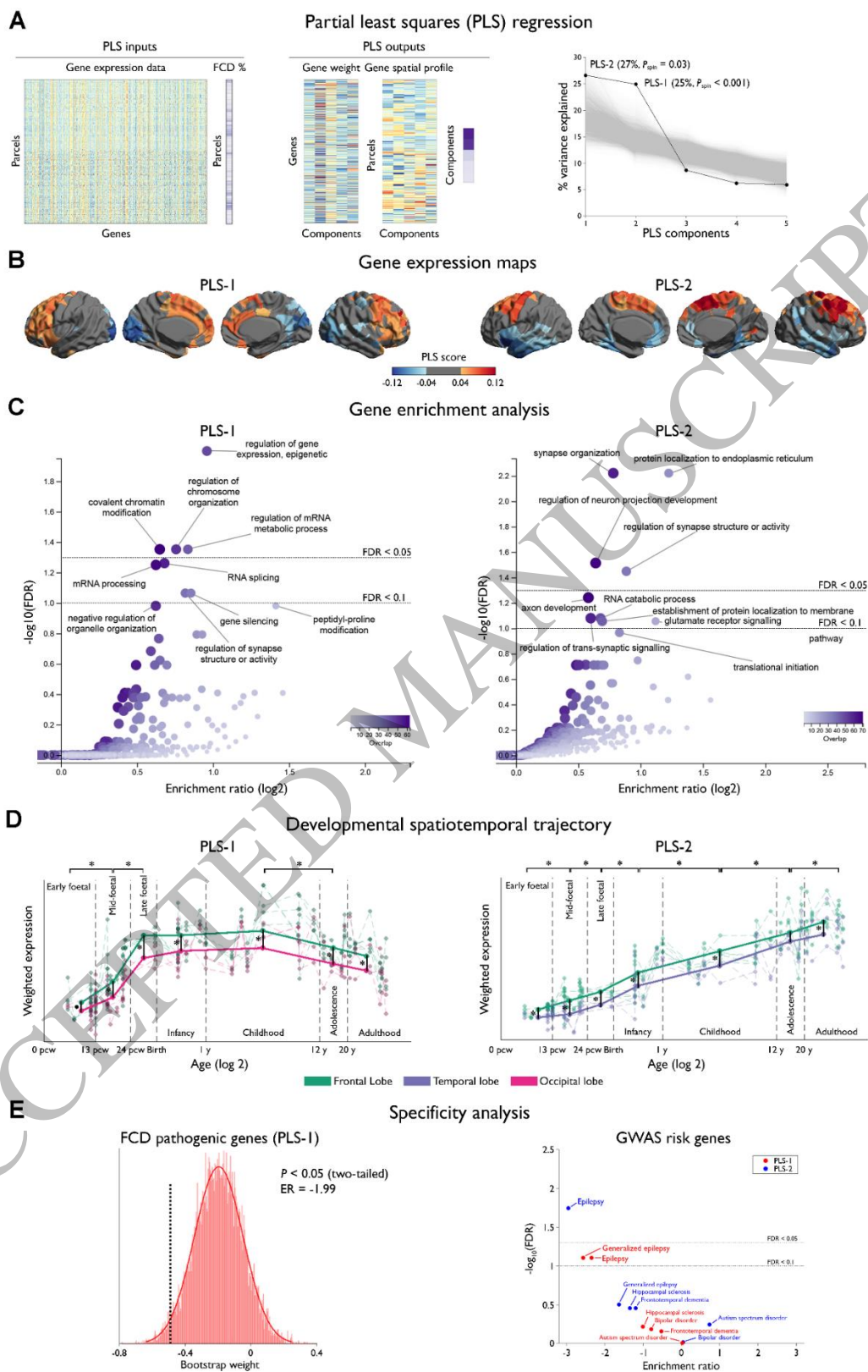


Figure 2
159x44 mm (x DPI)

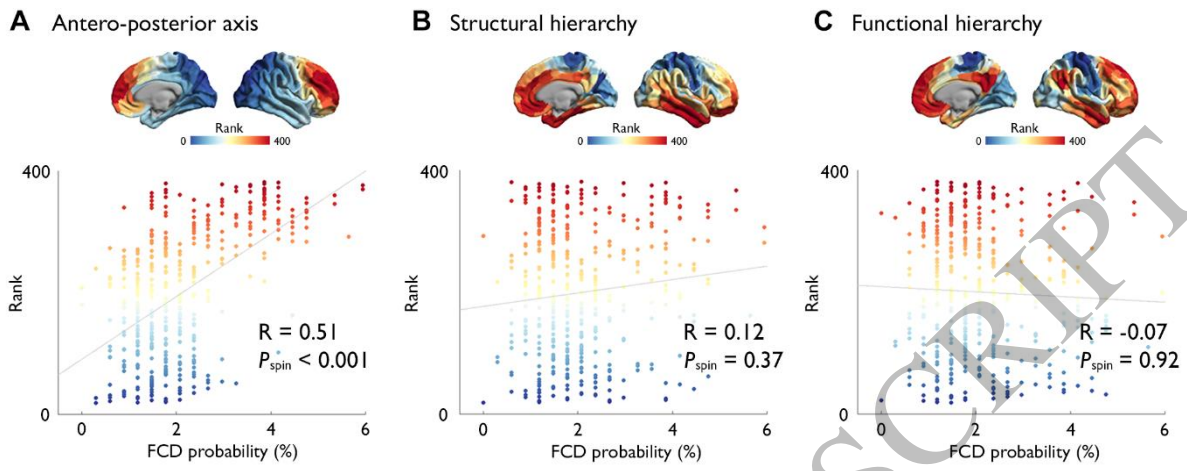
1
2
3
4



1
2
3

Figure 3
158x246 mm (x DPI)

1



2

3

4

Figure 4
159x63 mm (x DPI)

ACCEPTED MANUSCRIPT